

## Chapter 22

# Uniaxial Alignment of Electrospun Nanofibers

Dan Li, Jesse T. McCann, and Younan Xia\*

Department of Chemistry, University of Washington, Seattle, WA 98195

The conventional setup for electrospinning has been modified to generate uniaxially aligned arrays of nanofibers over large areas. By using a collector with conductive strips separated by an insulating gap of variable width, these arrays could be directly fabricated during the electrospinning process. Directed by electrostatic forces, the charged nanofibers were stretched across the gap in a uniaxially aligned fashion. It was also versatile to stack the nanofibers into multilayered architectures with well-controlled hierarchical structures by using multiple electrode pairs patterned on an insulating substrate. Both methods have been applied to nanofibers consisting of organic polymers, carbon, ceramics, and composites. The facile formation of uniaxially aligned arrays of nanofibers with controlled positions and orientations on a solid substrate makes it possible to fabricate electrospun nanofiber-based devices and systems.

## Introduction

Electrospinning represents a simple and versatile tool for manufacturing nanofibers (1,2). Besides polymers, this technique has recently been extended to produce carbon, ceramic, and composite nanofibers (1-3). Because of the bending instability associated with a spinning jet (4,5), electrospun fibers are often deposited on the surface of a collector (a piece of conductive substrate) as randomly oriented, nonwoven mats. Such mats are of great importance for applications in membrane separation and filtration, reinforcement of composites, texturing, sensing, scaffolding for tissue growth, enzyme immobilization and in electronic uses such as supercapacitors, actuators or photovoltaic devices (1,2). Many of the important applications of nanofibers, however, rely on the secondary and tertiary structures of these materials. For example, the fabrication of electronic and photonic devices often requires well-aligned and highly-ordered architectures (6-9). Even for fiber reinforcement and tissue engineering, uniaxial alignment of electrospun fibers is beneficial to improve their performance (10).

A number of approaches have been developed to fabricate electrospun fibers with well-ordered secondary structures. Alignment of electrospun fibers was observed by several groups when a cylinder with high rotating speed was used as the collector (10-12). Flow of air may also favor the orientation of fibers along the shearing direction (13). In order to improve the degree of orientation, Zussman and co-workers modified the design of a drum and used a tapered, wheel-like disk as the collector (14). It was found that most of the fibers could be collected on the sharp edge. The collected fibers were oriented parallel to each other along the edge. They further demonstrated that nanofiber crossbars could be readily fabricated using this collector (15). With the use of a similar setup, Natarajan, Xu, and coworkers have also fabricated well-aligned nanofibers (10,16). In addition to drums, metal or wooden frames have been explored by several research groups to collect electrospun nanofibers as relatively aligned arrays. Deitzel and co-workers have demonstrated that electrospun fibers could be aligned into parallel arrays using a multiple field technique (17), while Vaia and co-workers reported that they have fabricated aligned yarns of nylon-6 nanofibers by rapid oscillation of a grounded frame within the jet (18). Wendorff and co-workers have reported that they used a metal frame to collect parallel arrays of polyamide nanofibers (19). However, neither the mechanism of alignment nor a way to transfer the aligned fibers for use in the fabrication of devices has been reported.

We have recently demonstrated that uniaxially aligned electrospun nanofibers can be obtained by using a collector with an insulating gap (20,21). This method allows the fibers to be transferred or directly deposited onto a solid substrate for device fabrication. It is also convenient to fabricate multilayered

hierarchical structures of well-aligned nanofibers by using suitable electrode configurations.

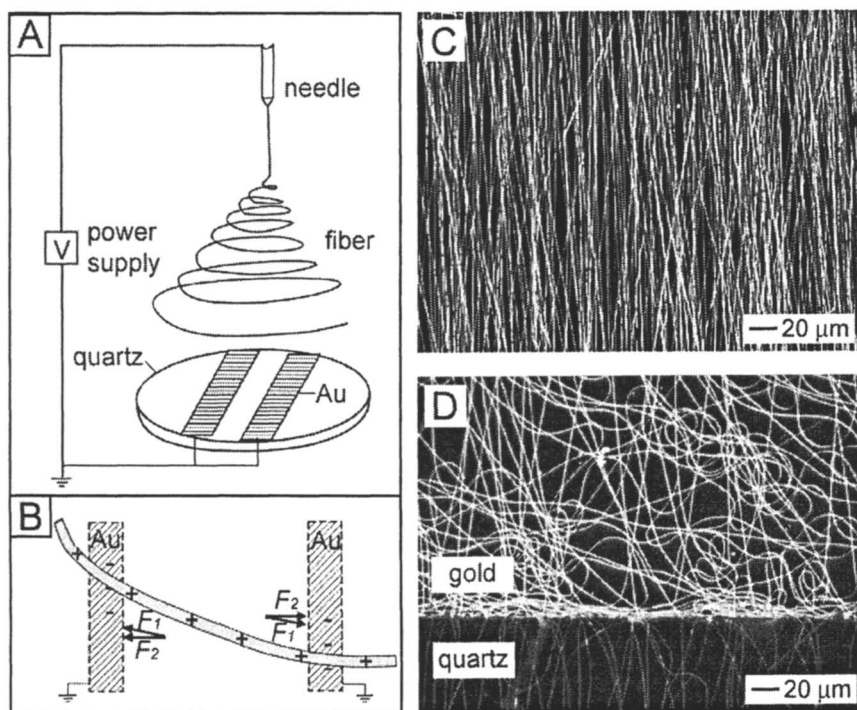
## Experimental

Figure 1A illustrates the schematic setup used for our electrospinning experiments. It is similar to the conventional one except for the use of two separated conducting strips as the collector. The collector could be fabricated from two pieces of conducting silicon wafers by separating with a void gap, or two conductive gold strips deposited on a quartz or plastic substrate by evaporation of gold through a physical mask. The gap width was fixed at 7 mm for our experiments, though the width could be varied from tens of micrometers to several centimeters. Poly(vinyl pyrrolidone) (PVP, Aldrich,  $M_w \approx 1,300,000$ ) was electrospun to demonstrate this concept. In a typical procedure, a 6 wt% solution of PVP in a mixture of ethanol and water (8:1.5 by volume) was loaded into a plastic syringe equipped with a stainless steel needle. The needle was connected to a high-voltage power supply (ES30P-5W, Gamma High Voltage Research Inc., Ormond Beach, FL) capable of generating up to 30 kV of DC voltage. The solution was continuously supplied using a syringe pump at a rate of 0.2 mL/h. The voltage used for electrospinning was 6 kV, and the collection distance was 9 cm. Optical micrographs (dark field mode) were recorded using a Leica microscope equipped with a digital camera. Scanning electron microscope (SEM) micrographs were obtained using a field-emission scanning electron microscope (Sirion, FEI, Portland, OR) operating at an accelerating voltage of 5 kV.

## Results and Discussion

### Uniaxial Alignment of Nanofibers

Figure 1B shows the electrostatic forces acting on a segment of charged nanofiber stretched across the gap. An electrospun fiber can be approximated as a string of positively (or negatively if a negative potential is applied to the solution) charged elements connected by a viscoelastic material. Near the point of collection, the nanofiber should experience two sets of electrostatic forces: The first set ( $F_1$ ) originates from the splitting electric field, while the second one is between the charged fiber and the induced image charges on the surface of the two grounded electrodes ( $F_2$ ). The electrostatic force  $F_1$  is parallel to the electric



**Figure 1.** A) Schematic illustration of the electrospinning setup used for fabricating uniaxially aligned arrays of nanofibers. The collector was composed of a quartz wafer patterned with a pair of gold electrodes. B) Analysis of the electrostatic forces operating on a charged nanofiber spanning across the gap.  $F_1$ : the electrostatic force directly acted by the electric field;  $F_2$ : the Columbic interactions between the positive charges on the nanofiber and the negative image charges on the two grounded electrodes. C) Optical micrograph of PVP nanofibers collected between a pair of gold electrodes patterned on a quartz wafer. The collection time was 20 seconds. D) Optical micrograph of the edge of a gold electrode. The collection time was 3 seconds.

fields and therefore pulls the ends of the fiber toward the grounded electrodes. Since Coulombic interactions are inversely proportional to the square of the separation between charges, the ends of the fiber closest to the grounded substrate will generate a strong electrostatic force ( $F_2$ ), which will stretch the nanofiber across the gap and thereby position it perpendicular to the edges of the electrode.

Figure 1C is a dark field optical micrograph of a portion of nanofibers that were deposited on top of a quartz gap. Figure 1D is an optical micrograph that shows the edge of one of the conductive strips. These figures clearly show that the fibers were aligned as a uniaxial array across the insulating gap, while the fibers that were deposited on the conductive strip were randomly oriented.

Both the degree of uniaxial alignment and the density of the fibers on the gap were dependent on the collection time. Figure 2 shows the effect of collection time on fiber alignment and density. Fibers collected for 1 second showed some alignment, though less than 50 percent of the fibers were aligned within  $10^\circ$  of normal. Fibers collected for 5 seconds had better alignment, with more than 60 percent of fibers aligned within  $10^\circ$  of normal. Fibers collected for 30 seconds exhibited much improved alignment, with over 80 percent of the fibers aligned within  $10^\circ$  of normal. From these images and statistical analysis of the angles between the long axes of the fibers, it can be observed that the degree of alignment increased with increasing collection time. This phenomenon was ascribed to the repulsions between charged fibers. Unlike fibers deposited onto an electrode (where the fibers were discharged immediately upon contacting with the electrode), the fibers suspended across the insulating gap remained highly charged. These fibers had the same charge and therefore repelled each other. This type of electrostatic repulsions also tended to make these fibers align in a parallel fashion since the parallel configuration represents the lowest energy state.

When a void gap was used, the aligned fibers suspended across this gap could be easily and conveniently transferred to the surface of a solid substrate for further processing or device fabrication by moving the substrate vertically through the gap after the nanofibers had been collected. The collector with a void gap is particularly useful to manipulating single electrospun fibers (for example, for fabricating single-fiber devices). By controlling the collection time, well-separated fibers could be suspended across the gap, and single fibers could be conveniently obtained by breaking other fibers. The fabrication of arrayed crossbar junctions by this method was facile. However, the void gap was not suited for collecting fibers with diameters less than 150 nm because such thin fibers could not support their own weight and broke when they were stretched across the gap. One could solve this problem by patterning metal strips on an insulating substrate. These patterned electrodes are particularly useful for fabricating multilayered nanofiber architectures with controllable orientations.

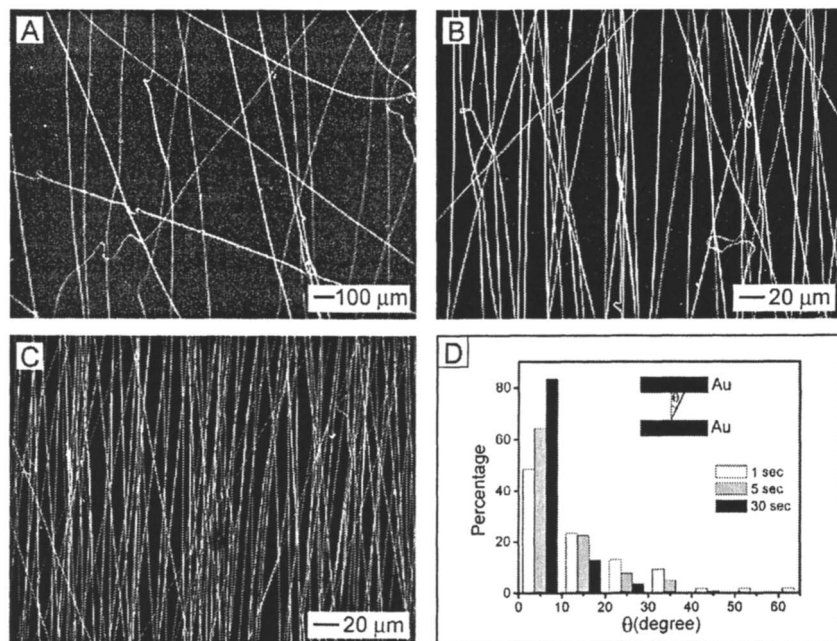


**Figure 2.** A-C) Typical optical micrographs of PVP nanofibers that were collected between two gold electrodes patterned on a quartz wafer. The collection times for the three samples were 1, 5, and 30 seconds, respectively. D) Distribution of angles between the long axis of a fiber and the normal to the edges of two parallel gold electrodes. The results displayed in each panel came from analysis of more than 150 fibers. Adapted in part from reference 21, © 2004 Wiley-VCH.

## Multilayered Structures of Aligned Nanofibers

Uniaxially aligned arrays were only formed between the electrodes, thus their spatial orientation and position could be controlled by the location and configuration of the grounded electrodes. It was very convenient to stack the nanofibers into multilayered hierarchical structures by using multiple electrode pairs patterned on an insulating substrate. Figure 3A shows a schematic illustration of the four-electrode pattern that was deposited on a quartz wafer. When only one pair of electrodes (1-3 or 2-4) was grounded, the spun fibers were deposited solely on the grounded electrode pair and the gap between them.

By alternately grounding the electrode pairs, a double-layer mesh of fibers could be obtained, as the optical micrograph illustrates (Figure 3B). A six-electrode pattern was also used, as shown in Figure 3C. By alternately grounding the electrode pairs (1-4, 2-5, and 3-6), a tri-layered mesh was generated by the sequential deposition of three layers of uniaxially aligned nanofibers, with their long axes rotated by  $60^\circ$ . It is believed that architectures of greater complexity could be generated by controlling the electrode configuration and the sequence of voltage application.

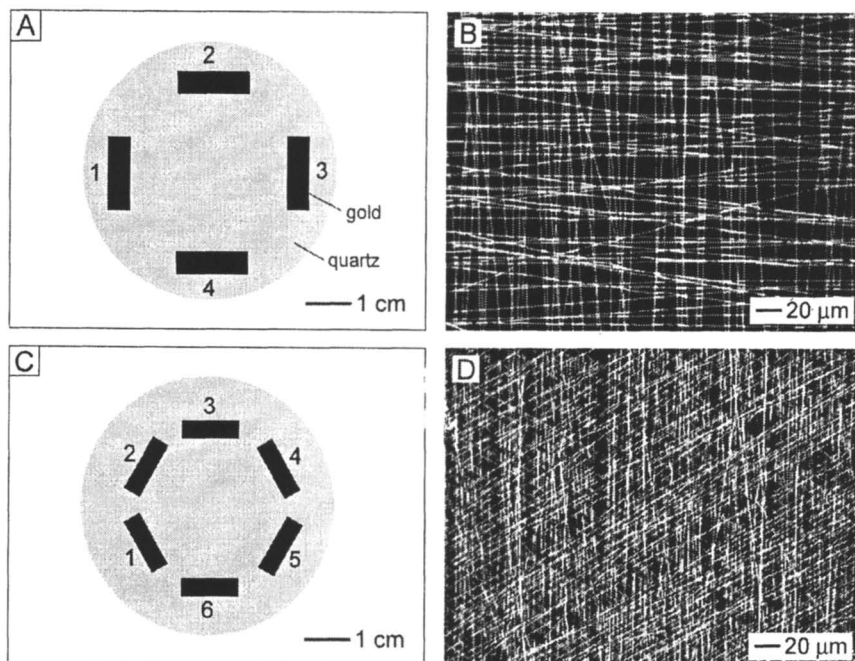


*Figure 3. A, C) Schematic illustration of test patterns that were composed of four and six electrodes deposited onto quartz wafers. B, D) Optical micrograph of a mesh of PVP nanofibers collected in the center region of the gold electrodes shown in (A) and (C), respectively. During collection, the opposing electrode pairs were alternately grounded for ~5 seconds. Adapted in part from reference 21, © 2004 Wiley-VCH.*

It is quite remarkable that this technique allows for the alignment and assembly of nanofibers into complex architectures concomitant with the fabrication of the fibers. By using and extending these electrode designs,

multiple layers of well-aligned nanofibers with different compositions could be readily assembled to create well-ordered hierarchical architectures on a solid substrate. Such structures could find immediate use in the fabrication of both electronic and photonic devices. In addition, different arrays of nanofibers can be integrated into the same device, since a large number of electrode patterns can be readily fabricated on a substrate using conventional microfabrication methods.

### Uniaxially Arrayed Fibers of Various Materials

We have successfully used the setup shown in Figure 1A to fabricate uniaxially aligned nanofibers from a variety of organic polymers including poly(ethylene oxide), polystyrene, polyacrylonitrile and polycaprolactone. Our results indicate that this approach is a generic one which can be used for many types of conventional organic polymers. We have also been able to extend the conventional electrospinning technique to fabricate functional ceramic nanofibers by spinning polymer solutions containing sol-gel precursors, followed by calcination of as-spun composite nanofibers at elevated temperatures (20-23). Hollow nanofibers have also been fabricated using a dual-capillary spinneret system (24). All of these fibers could also be collected as uniaxially aligned arrays using a collector with an insulating gap. Figure 4 shows some representative SEM images of aligned nanofibers made of different materials. In addition to pure polymer or ceramic nanofibers, organic functional molecules, biological macromolecules, nanoparticles, inorganic nanowires and carbon nanotubes could also be incorporated into solutions for electrospinning of functionalized nanofiber arrays. These aligned arrays of nanofibers with various functionalities hold much promise as building blocks for the fabrication of nanoscale devices.

### Properties and Applications of Uniaxially Aligned Nanofibers

The fabrication of uniaxially aligned arrays by electrospinning allows for the exploration of a range of interesting properties and applications associated with one-dimensional nanostructures. As an example, the controlled alignment of nanofibers should result in the formation of nanostructured materials with highly anisotropic behavior. The electrical conductivities of thin films of uniaxially aligned nanofibers of both carbon and  $\text{SnO}_2$  were found to be highly anisotropic. The ratio between the conductivities parallel and perpendicular to the long axis of the fiber was  $\sim 15$  for a film with a density of  $\sim 900$  nanofibers per millimeter.



Using a collector with a void gap, it was very convenient to collect single fibers for device fabrication. Compared with 1D nanostructures prepared by

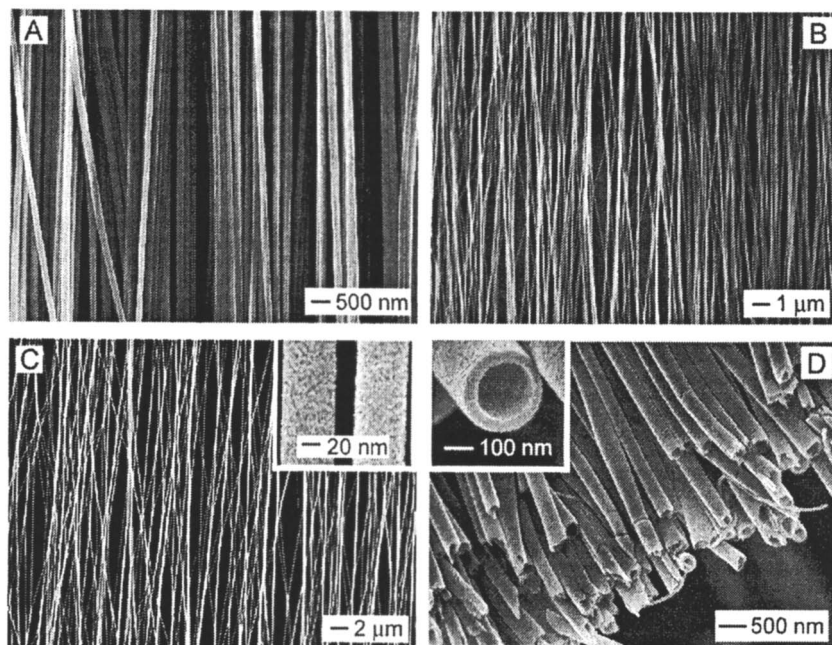


*Figure 4. SEM images of uniaxially aligned nanofibers (A-C) and nanotubes (D) with various compositions: A) carbon; B)  $\text{TiO}_2$ /PVP composite; C) Sb-doped  $\text{SnO}_2$ ; and D) anatase.*

other chemical or physical methods, it was much easier to collect and manipulate single nanofibers. Figure 5A shows the SEM image of an individual Sb-doped nanofiber that was collected on top of a gap and subsequently transferred onto two gold electrodes separated by  $\sim 20\ \mu\text{m}$ . The inset shows a nonlinear current-voltage curve measured from this nanofiber, which shows behavior similar to that of a metal oxide varistor.

Uniaxially aligned nanofibers also have the potential to be good optical polarizers. The Maxwell-Garnett model predicts that the attenuation of light is greater for the electric field polarized parallel to the long axis of an infinite cylinder than the component perpendicular to the axis (25,26). Our results agree well with the Maxwell-Garnett model. Figure 5B shows Rayleigh scattering spectra of a parallel array of PVP nanofibers. It can be seen that the extinction of

incident light with polarization parallel to the long axis was three times greater than the extinction of light polarized perpendicular to the long axis of the fibers.

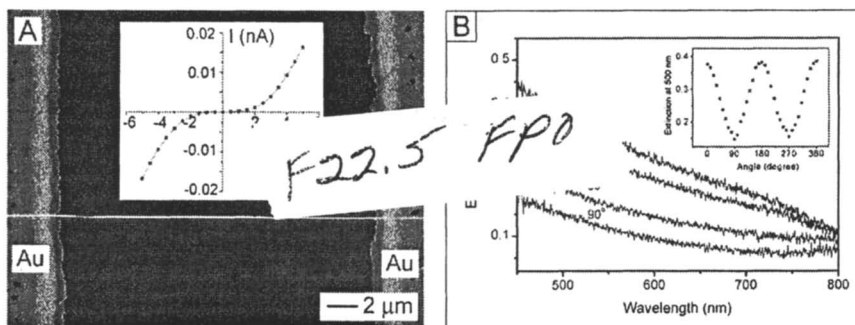


**Figure 5.** (A) SEM image of a single Sb-doped  $\text{SnO}_2$  nanofiber stretched across two gold electrodes. The inset shows a typical I-V curve measured from the device. (B) Rayleigh scattering spectra obtained from a uniaxially aligned array of 90-nm PVP nanofibers with the polarizer oriented at various angles relative to the longitudinal axes of the nanofibers. The inset shows how the extinction at 500 nm was modulated (as a cosine wave) as a function of the angle between the nanofibers and the polarization.

## Conclusion

By using collectors with an insulating gap, the electrospinning process has been modified to provide a simple and versatile method for creating uniaxially aligned arrays of nanofibers with various compositions and properties. The use of electrodes with insulating gaps between pair-wise plates allowed for the uniaxial alignment of fibers into parallel arrays via electrostatic forces. It was also possible to stack the aligned nanofibers into multilayered films with well-defined hierarchical structures by controlling the configuration for patterned electrodes. This system holds much promise for the fabrication of electrospun nanofiber-based architectures, devices, and systems.

## References

1. Reneker, D. H.; Chun, I. *Nanotechnology* **1996**, *7*, 216.
2. Li, D.; Xia, Y. *Adv. Mater.* **2004**, *4*, in press.

3. Larsen, G.; Velarde-Ortiz, R.; Minchow, K.; Barrero, A.; Loscertales, I. G. *J. Am. Chem. Soc.* **2003**, *125*, 1154.
4. Reneker, D. H.; Yarin, A. L.; Fong, H.; Koombhongse, S. *J. Appl. Phys.* **2000**, *87*, 4531.
5. Shin, Y. M.; Hohman, M. M.; Brenner, M. P.; Rutledge, G. C. *Polymer* **2001**, *42*, 9955.
6. Kovtyukhova, N. I.; Mallouk, T. E. *Chem. Eur. J.* **2002**, *8*, 4354.
7. Huang, Y.; Duan, X.; Wei, Q.; Lieber, C. M. *Science* **2001**, *291*, 630.
8. Favier, F.; Walter, E. C.; Zach, M. P.; Benter, T.; Penner, R. M. *Science* **2001**, *293*, 2227.
9. Melosh, N. A.; Boukai, A.; Diana, F.; Gerardot, B.; Badolato, A.; Petroff, P. M.; Heath, J. R. *Science* **2003**, *300*, 112.
10. Xu, C. Y.; Inai, R.; Kotaki, M.; Ramakrishna, S. *Biomaterials* **2004**, *25*, 877.
11. Kim, J.-S.; Reneker, D. H. *Polym. Eng. Sci.* **1999**, *39*, 849.
12. Kameoka, J.; Craighead, H. G. *Appl. Phys. Lett.* **2003**, *83*, 371.
13. Chun, I.; Reneker, D. H.; Fong, H.; Fang, X.; Deitzel, J.; Tan, N. B.; Kearns, K. *J. Adv. Mater.* **2003**, *31* (1), 37.
14. Theron, A.; Zussman, E.; Yarin, A. L. *Nanotechnology* **2001**, *12*, 384.
15. Zussman, E.; Theron, A.; Yarin, A. L. *Appl. Phys. Lett.* **2003**, *82*, 973.
16. Sundaray, B.; Subramanian, V.; Natarajan, T. S. *Appl. Phys. Lett.* **2003**, *82*, 973.
17. Deitzel, J. M.; Kleinmeyer, J. D.; Hirvonen, J. K.; Tan, N. C. B. *Polymer* **2001**, *42*, 8163.
18. Fong, H.; Liu, W. D.; Wang, C. S.; Vaia, R. A. *Polymer* **2002**, *43*, 775.
19. Dersch, R.; Liu, T.; Schaper, A. K.; Greiner, A.; Wendorff, J. H. *J. Polym. Sci. A* **2003**, *41*, 545.
20. Li, D.; Wang, Y.; Xia, Y. *Nano Lett.* **2003**, *3*, 1167.
21. Li, D.; Wang, Y.; Xia, Y. *Adv. Mater.* **2004**, *16*, 361.
22. Li, D.; Xia, Y. *Nano Lett.* **2003**, *3*, 555.
23. Li, D.; Herricks, T.; Xia, Y. *Appl. Phys. Lett.* **2003**, *83*, 4586.
24. Li, D.; Xia, Y. *Nano Lett.* **2004**, *4*, 933.
25. Rogers, J. A.; Paul, K. E.; Jackman, R. J.; Whitesides, G. M. *Appl. Phys. Lett.* **1997**, *70*, 2658.
26. Aspnes, D. E. *Thin Solid Films* **1982**, *89*, 249.